XMaS NEWSLETTER

2005

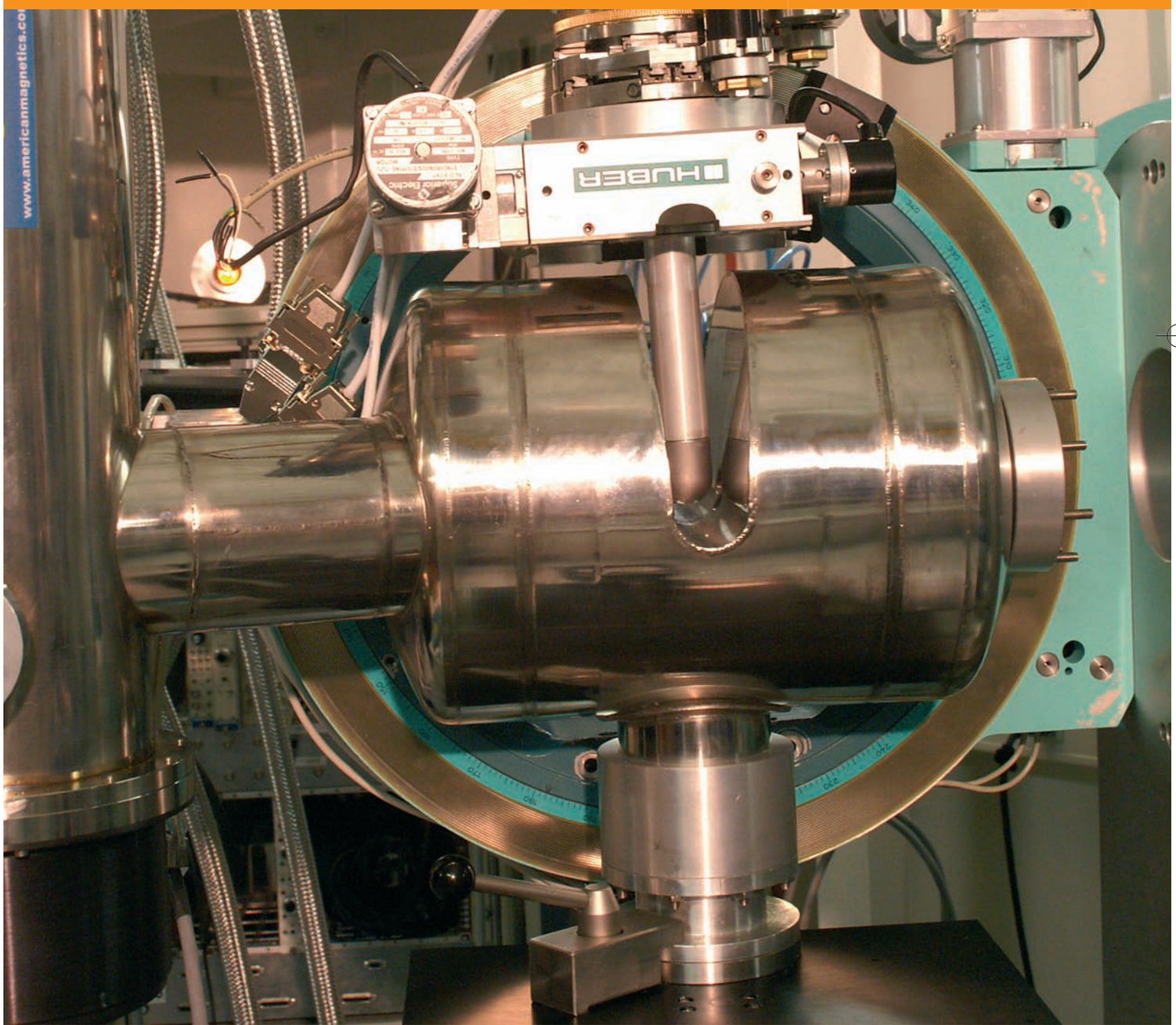

XMaS the UK-CRG

contents

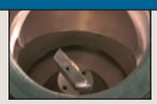

Status

The year 2005 ended with the long-awaited delivery of the 4T magnet, just before Christmas. Delivery would have occurred sooner but for a hiccup following first assembly and test of the magnet. This revealed a thermal shortcircuit to the welded stainless containment vessel which had to be disassembled in order to correct the fault. Understandably, this introduced a delay of several weeks. But the good news is that the problem was solved, the magnet functions magnificently and is already in use on the beamline – a unique facility given the field/angular-access capability. More details are given in the article, under Instrumental Developments, on page 4.

The diamond phase plate flipper project has made progress since the report in the article in the previous Newsletter. We have now run a trial of a prototype flipper assembly, provided by the Functional Materials Group at the NPL, together with the necessary electronics, some purchased and much loaned. This first trial yielded much to encourage us and is more fully reported, also under instrumental developments, on page 4. We have scheduled a full test experiment in the current scheduling period, in order to understand better the operational capabilities of the system, before offering this to our user community.

A further item reported under Instrumental Developments, on page 5, is the projected orbit-plane monitor. This has been craftily designed to fit into a space upstream of the monochromator, currently occupied by a bellows assembly. Unforeseen in the original design of the beamline, it has been necessary to contemplate retrofitting this device because of unanticipated beam movements, the lack of sensitivity of the existing upstream monitor and the particular sensitivity that phase plate set-ups have to quite small beam movements.

This will be the last newsletter before we submit an application for renewed funding beyond the current contract, due to end in September 2007. It is, thus, very important for us to be able to present the best and most comprehensive publication list for all who have used the XMaS beamline. So, to assist us present the best case for continuation, would you check that Sandra Beaufoy at Warwick has the most up-to-date information about your publications and, of course, expedite any you may have still in preparation. ■

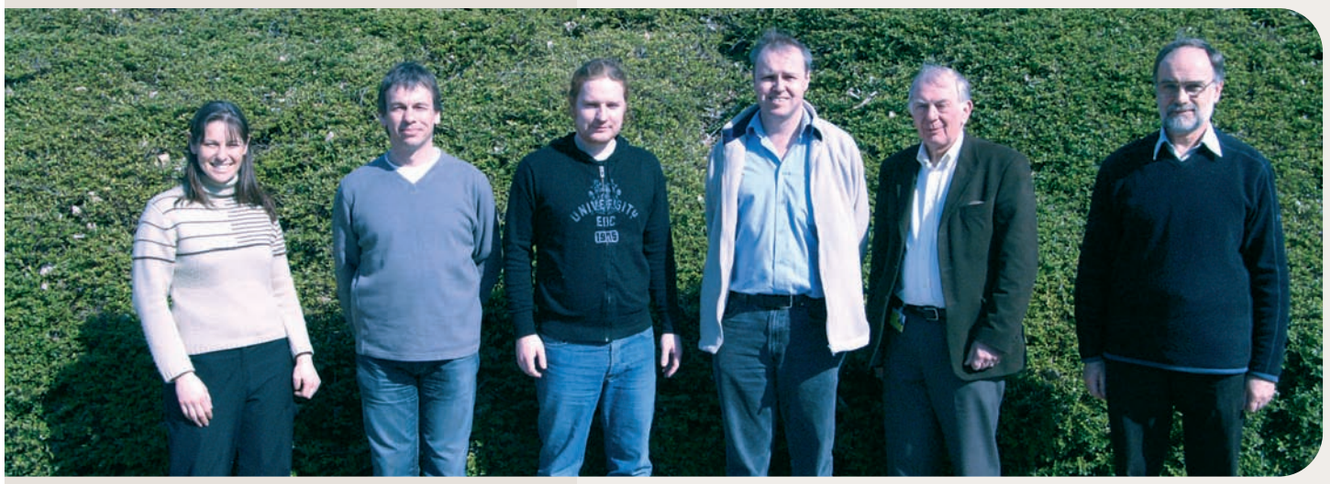

The ESRF in February and XMaS in May

The annual XMaS Users' Meeting was held in the Department of Physics at the University of Warwick on Thursday 26th May 2005. The meeting attracted approximately 40 participants representing 13 UK institutions, including a sizeable Liverpool contingent who the previous evening had been celebrating the success of the football team in winning the European Cup (aka Champions League)! After a welcome by Malcolm Cooper, the meeting began with presentations by the beamline staff covering beamline operation (David), development of the piezoelectric polarisation flipper (Laurence), advances in the software for the MAR detector (Danny) and a range of other technical development projects (Paul). Three scientific presentations completed the morning session; Tom Beale (Durham) described charge orbiting and orbital ordering in bilayer mangenites, Paul Strange (Keele) described the theory of resonant x-ray scattering and finally Danny Mannix (XMaS) presented recent measurements of magnetic order in $CeLaB_6$ compounds. After an excellent lunch and a viewing of the posters, the scientific presentations continued with Emyr Macdonald describing the use of the MAR detector for studying semiconducting polymers. Jon Goff (Liverpool) presented a combined x-ray and neutron study of magnetic nanoparticle assemblies and Tom Hase (Durham) continued the nanoparticle theme, describing measurements of the x-ray scattering from magnetic nanodot arrays. Finally Steve Collins (DIAMOND) presented an amusing comparison between Diamond and the ESRF and demonstrated how the Materials and Magnetism beamline at DIAMOND (I16) will complement the XMaS beamline in the future. The meeting concluded with a brief discussion of the next XMaS grant application during which it was noted that both the quality and diversity of the science that is being performed on the beamline continue to grow. The poster prize went to Ben Fowler (Liverpool) for his work on the effects of temperature on the atomic structure at the electrochemical interface.

Top: *Ben Fowler from Liverpool holding his prize in front of his winning poster.*

Bottom: *Tom Hase in front of the winning poster from Durham in the ESRF's user meeting poster competition. The object in Tom's hand is not thought to be the prize awarded by the ESRF!*

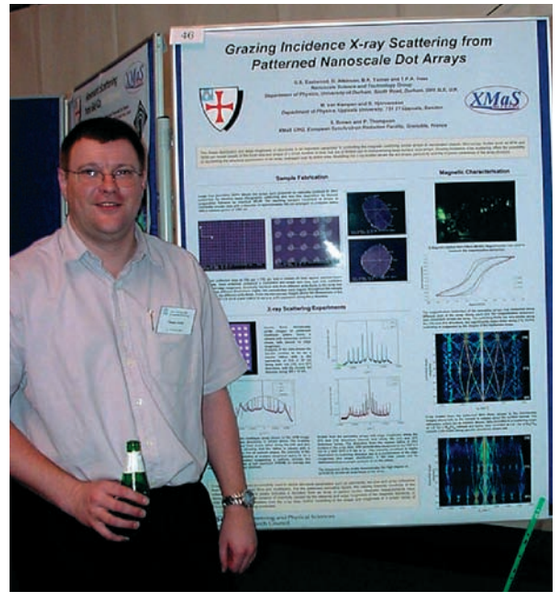

The 4 Tesla magnet

The magnet has at last been delivered, arriving on the beamline just before Christmas after acceptance tests at the manufacturer's site in Tennessee. It was demonstrated that the magnet could achieve a field of 4.4 Tesla before quenching, thus the design goal of 4.0 Tesla is adequately met and this will be the operational maximum field.

The rated field of the magnet at an operating temperature of 4.2 K is 4 Tesla, with a homogeneity of +/-1 % in a 1 cm diameter sphere at an approximate operating current of 80 Amperes. Great care had been taken during this programme to ensure the magnet would fit into the diffractometer without interference and allowing maximum access for incident and reflected x-ray beams. This included the supply of a plastic replica model at an early stage to avoid expensive errors later. Figure 1 shows the magnet installed on our Huber diffractometer with the field transverse to the x-ray beam. As explained in our 2003 issue of the Newsletter, the magnet can also be mounted with the field vertical and also co-axial with the beam – all these orientations have been verified.

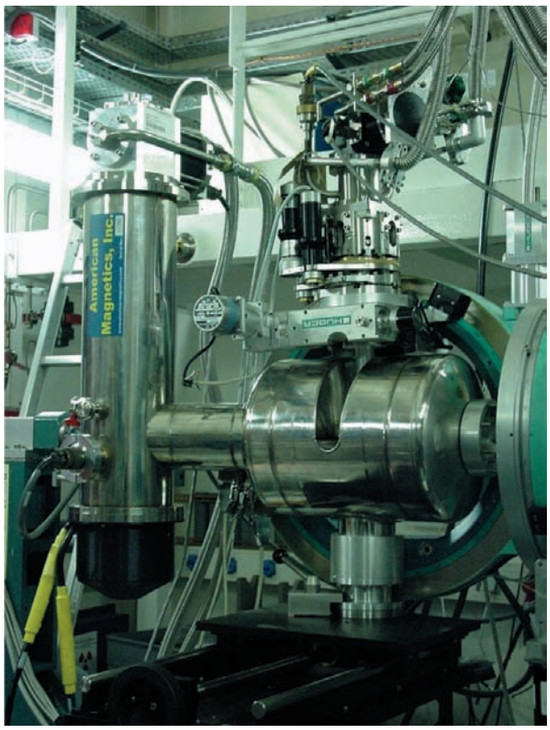

Figure 1: *The 4T magnet installed on the XMaS Huber diffractometer.*

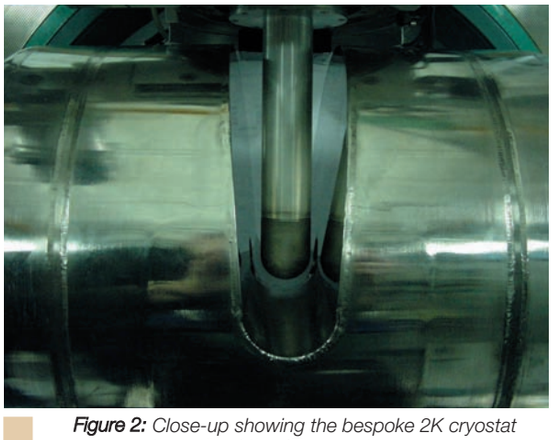

Figure 2: *Close-up showing the bespoke 2K cryostat between the coils of the 4T magnet.*

Earlier last year we took delivery of its companion sample cryostat. This small-aspect variable temperature insert is based around a commercial two-stage displex, capable of reaching 10K. A third stage, developed by the cryogenics group at the ILL, in Grenoble, has been added. This novel device is capable of operating down to ~2K using ^{4}He gas and may be operated over a wide range of angles without degradation of the base temperature. It is envisaged that the cryostat will achieve a temperature of ~1K when used with ^{3}He gas.

At the time of writing the magnet/cryostat combination has been used for two user experiments, in addition to the experiments reported by team members on pages 12 and 13 of this issue, and we have others scheduled in the current period. We look forward to including highlights of these and other experiments performed with the magnet in the next issue of the Newsletter.

Diamond phase plate flipper

The XMaS beamline is now capable of rapidly switching the polarisation of the x-ray beam transmitted by the diamond phase plate from left to right circular. This has been made possible thanks to the work undertaken by the NPL's Functional Materials Group who designed a novel piezo driven device capable of reversing the photon helicity at up to 150 Hz. The prototype, Figure 1, uses two pairs of multilayer piezoelectric stacks mounted on opposite sides of, and coupled to, an aluminium plate through two weak links. They are driven in opposite directions to provide an angular displacement of up to 350 arc seconds. The compact assembly allows easy mounting on the phase plate Huber 410 circle. The diamond is attached to a small copper goniometer which screws directly into the aluminium plate.

The performance of the flipper was tested under real conditions by measuring the XMCD signal of a $GdCo_2$ foil at the L_2 edge of gadolinium. A sinusoidal function generator was used to drive the piezoelectric stacks in phase quadrature and to provide a reference signal to a lock-in amplifier. The diamond was rotated at 10 Hz. The incident and transmitted intensities were measured with ionisation chambers and the resulting currents were amplified and converted to voltages. A log divider normalised the intensity from the sample to that transmitted from the diamond. The resultant signal was then fed to the lock-in amplifier. The dichroic signal was then measured from the lock-in output synchronized to the flipping of the helicity.

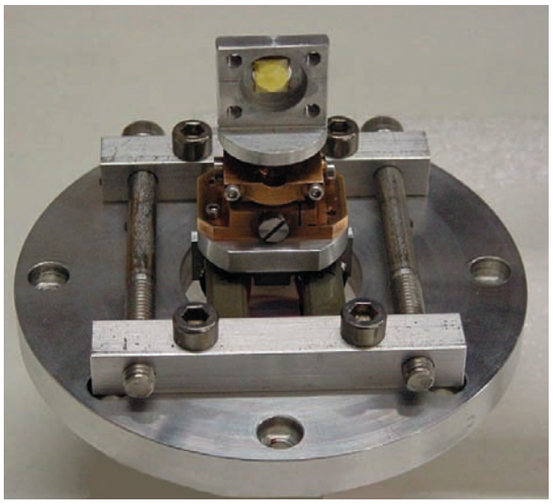

Figure 1: The prototype flipper assembly. The diamond phase plate is the yellow crystal at the top of the picture.

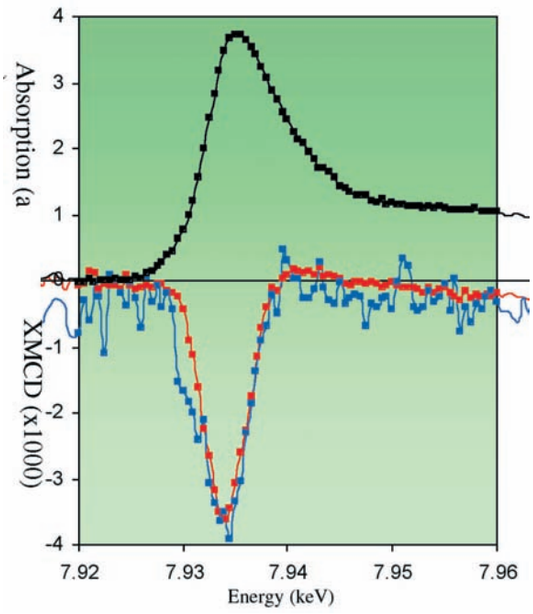

Figure 2: XMCD measurements performed on a $GdCo_2$ foil at the Gd L_2 edge with the flipper (red curve) and the standard method (blue curve).

Figure 2 shows the XMCD signal measured with the flipper (red curve) and compared to that measured with the standard method (blue curve) with the same counting time. As expected, the signal to noise ratio is considerably lower using the lock-in detection. Although the lock-in worked reasonably well when a dichroic signal was present, we observed that it struggled to "lock-in" away from the edge. Further commissioning will be required, notably to improve the lock-in detection.

Orbit-plane monitor

A bending magnet source produces a horizontal fan of synchrotron radiation which is highly linearly polarised in the orbital plane and tends to circular polarisation as viewed further above or below the plane. Some experiments, especially those that make use of a diamond phase plate, are very sensitive to changes of the beam polarisation, as caused typically by movements of the x-ray beam. It is, therefore, useful to know accurately the position of the beam at any time. Although each beamline is equipped with a beam position monitor (BPM), situated upstream of the shield wall, it is often difficult to correlate movements reported by this with the change of intensity/ polarisation observed at the sample position. We have evolved a procedure whereby a monitor is mounted in the experimental hutch to view the beam, scattered horizontally, whilst scanning a narrow slit aperture vertically through the white beam. This method, however, is disruptive of the experimental setup and, thus, the progress of the experiment. We have now designed a new system for monitoring the whitebeam, mounted in a short orbit vessel (Figure 1) to be installed permanently between the primary slits and the monochromator. It consists of a motorised water-cooled copper block, which can be driven to intercept and scatter the beam horizontally through 90° and the intensity monitored with a photodiode. It will also be possible to drive a range of attenuators into the beam which can assist future studies on monochromator heat-load for the projected upgrade of the ring current. ■

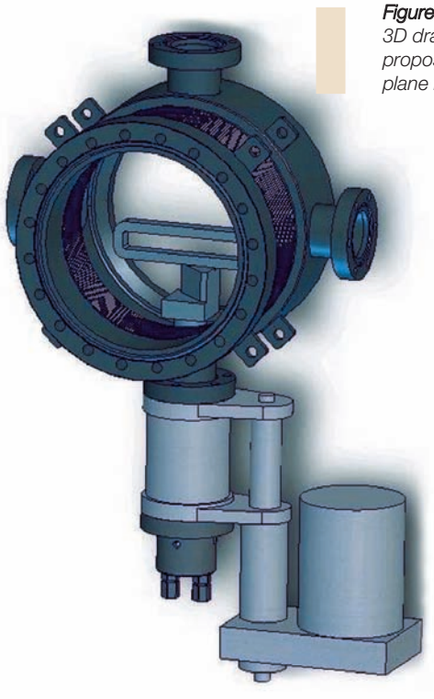

Figure 1: 3D drawing of the proposed orbit-plane monitor.

Ordering of conjugated polymers for organic transistors

A. Das, H.E. Thomas, H. Simmonds, M.L. Turner and J.E. Macdonald – for further information contact J.E. Macdonald at Dept. of Physics & Astronomy, University of Wales, Cardiff.
macdonald@cf.ac.uk

Organic thin-film transistors are potential low-cost alternatives to mainstream amorphous silicon-based technologies for large-area devices, e.g. displays and sensors, and low-end electronics, e.g. radio frequency identification tags and smart cards. Their compatibility with plastic substrates has rendered them ideal for creating compact, lightweight, mechanically flexible, and structurally inspiring electronic device designs (e.g. electronic papers) and can be prepared with low-cost liquid deposition techniques. Charge transport in organic semiconductors is dominated by hopping and hence molecular ordering, particularly in the channel at the interface with the gate dielectric, is crucial to achieving high charge carrier mobility. Liquid-crystalline conjugated polymers provide relatively strong molecular ordering and ease of thin-film preparation by spin-coating.

Grazing incidence diffraction provides an ideal technique to characterise the degree of structural order in thin films, particularly at the surface and potentially at a buried channel-gate dielectric interface. We report here GIXRD measurements on a solution-processable regioregular polythiophenes, poly(3,3'''-dialkyl-quaterthiophene), (PQT-12), (Fig. 1 (a)). Thin films of thickness around 6 nm were spin-cast from toluene solution onto Si/SiO_2 substrates treated with octadecyltrichlorosilane (OTS), which renders the oxide surface hydrophobic. Films for two molecular weights of 5,000 and 16,000 were compared. For the low molecular weight films, wellordered structures were obtained on spin-coating without annealing (Fig 1(b)). By varying the incident angle α, the effect of the surface on crystallinity can be determined (Figure 1(b-c)): the surface is more polycrystalline than the bulk of the film, which could be detrimental to mobility in the channel of a transistor. Molecular weight has a marked effect on structure: the higher molecular weight film structures are more disordered on spin-coating (Fig 1 (c)). Molecular weight has been observed to have a strong effect on ordering during in-situ annealing and these differences are being investigated further. The ability to monitor kinetic effects in polymer films has been significantly enhanced by the MAR area detector: full scans of relevant areas of reciprocal space can now be measured with a count time of 5 seconds for a 5 nm thick film, allowing both surface effects and kinetic effects to be measured with excellent time-resolution.

(a)

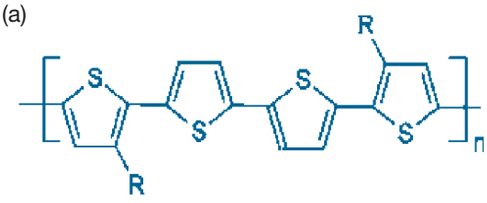

(b)

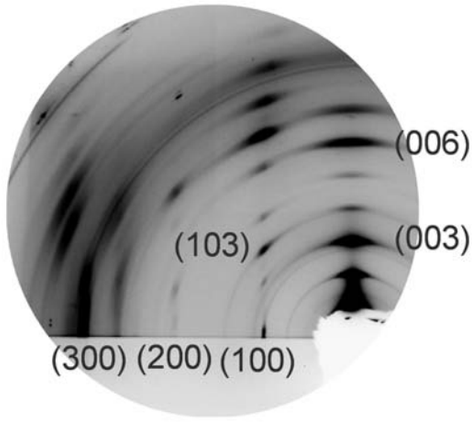

(c)

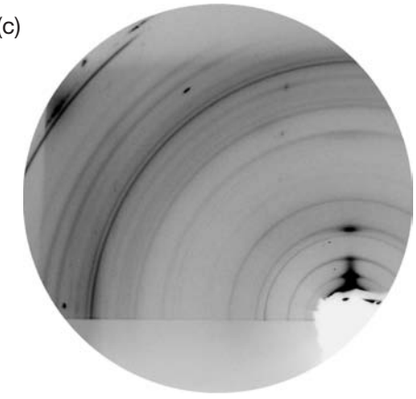

(d)

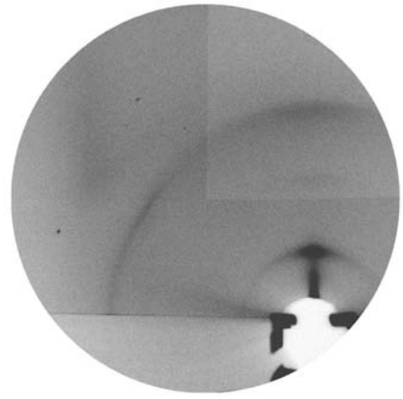

Figure 1 (a): *the chemical structure of regioregular poly(3,3'''-dialkyl-quaterthiophene), (PQT-12) of M_n = 16,000 (b) the diffraction pattern for incident angle α = 0.16° with a limited set of peaks indexed for clarity (c) the corresponding pattern for α = 0.06° (d) the diffraction pattern at α = 0.16° for M_n = 5,000.*

Two-dimensional mapping of texture in human dental enamel

M. Al-Jawad, S.H. Kilcoyne, D. Wood, R.C. Shore, R. Cywinski and L. Bouchenoire –
for further information contact M. Al-Jawad at School of Physics and Astronomy, University of Leeds, Leeds, LS2 9JT, UK.
m.al-jawad@leeds.ac.uk

Dental enamel is the most highly mineralised and strongest biological hard tissue. It comprises 95% hydroxyapatite (HA) mineral, 5% water, and 1% organic matter (noncollegenous protein). The hydroxyapatite crystal structure of dental enamel has been determined previously by several workers. HA has space group P63/m with lattice parameters a=9.513Å and c=6.943Å. In all previous reports, the measurements were made on powdered enamel collected from many teeth, therefore any texture information regarding the growth of the HA crystallites was lost. This information however is extremely valuable in the understanding of the formation of enamel, and in improved design of dental composites for restorations. We have recently performed an experiment on XMaS which for the first time maps the change in preferred orientation as a function of position in an intact section of tooth. We used the MAR ccd area detector to collect diffraction images every 50-300μm from sections of teeth ~500μm in thickness. An example of a 2-D map is shown in Figure 1.

The regions of highly crystalline enamel and poorly crystalline dentine are clearly visible. Additionally, it can be seen that below the groove between the two tooth cusps (the fissure), there is a circular region of enamel which is less crystalline than the surrounding structure. We believe this to be caused by a fissure lesion in the enamel which has affected the crystalline structure of the enamel. This type of lesion is undetectable by inspection of a whole tooth that has not been sectioned.

Diffraction patterns generated using fit2D from images b) and d) in Figure 1 are shown in Figure 2. Two orthogonal peaks 002 and 310 are marked in order to compare their peak intensities. In polycrystalline HA the value of the ratio of 002/310 should be between 2-3. In this highly textured enamel, the value of 002/310 varies enormously between 0.14(3) for Fig 2 ii) and 92.6(1) for Fig 2 iii). We are currently using Rietveld refinement of each diffraction pattern with texture parameters included to produce a complete 2-D texture map of healthy tooth enamel. Preliminary results suggest that the texture direction follows the shape of the enamel-dentine junction. This method will be used to investigate the changes that take place in the structure of enamel in carious (decayed) regions, and in teeth with genetic defects.

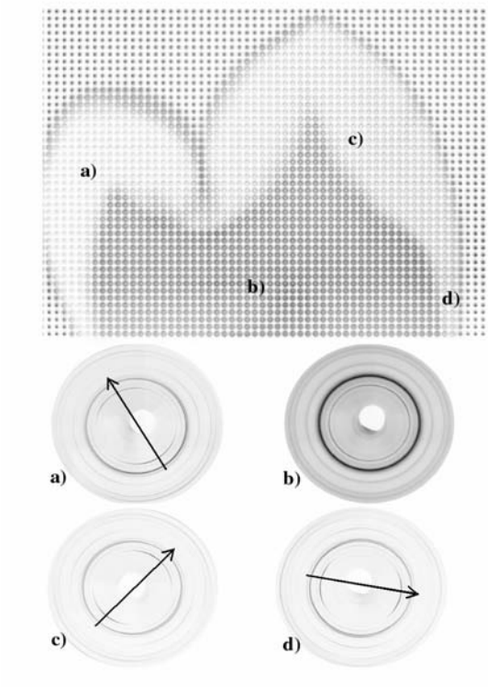

Figure 1: 2D image of whole tooth section of a healthy second molar. Diffraction images were collected every 150 μm. a), c) and d) illustrate the change in texture direction at difference positions within the enamel. b) shows the poorly crystalline nature of dentine.

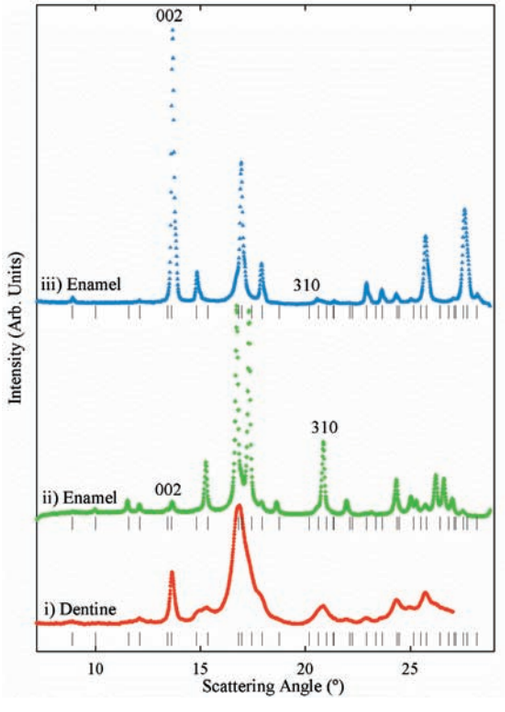

Figure 2: Diffraction patterns generated from 2D images. Each pattern is a 20° cake slice of the full 360° images. i) poorly crystalline dentine (at position b) in Fig 1), from 2θ=-10° to 10° ii) enamel at position d) in Fig 1) from 2θ=-10° to 10° and iii) enamel at position d) in Fig 1) from 2θ=80° to 100°.

Magnetic order in thin films of the heavy fermion superconductor UNi_2Al_3

M. Jourdan, Z. Zakharov, H. Adrian, A. Hiess, T. Charlton, N. Bernhoeft, D. Mannix – for more information contact: M. Jourdan, Joh.-Gutenberg-Universität, Mainz, Germany.
jourdan@uni-mainz.de

The isostructural (hexagonal, P6mmm) magnetic superconductors UPd_2Al_3 (T_N = 14K, T_{sc} = 2K) and UNi_2Al_3 (T_N = 7K, T_{sc} = 1K) both exhibit the coexistence of superconductivity and magnetic order at low temperatures. Understanding the interplay between magnetism and superconductivity is an area of active debate in condensed matter physics. Whereas for UPd_2Al_3 there is evidence by tunnel spectroscopy and inelastic neutron scattering for a magnetic Cooper-pairing interaction, in UNi_2Al_3, where the study of superconductivity is less advanced, already there are indications of important differences: Notably, in contrast to UPd_2Al_3 there are signs for a superconducting spin triplet state in UNi_2Al_3.

Neutron diffraction shows UPd-$_2Al_3$ to exhibit commensurate magnetic order as described by a propagation vector QUPA = (0 0 1/2) and the ordered moments of 0.85μB lie parallel to the a-axis. In UNi_2Al_3 not only the magnetic ordering temperature is lower, but the moment also smaller ($0.2\mu_B$) and the magnetic structure as determined in bulk single crystals has an incommensurate propagation vector Q_{UNA} = (0.39 0 1/2). This magnetisation density wave is amplitude modulated with the magnetic moments parallel to a*.

Recently we have been able to prepare superconducting epitaxial thin films of UNi_2Al_3 which grow with the a*-axis perpendicular to the substrate surface. We intend to investigate its superconducting properties by tunnel spectroscopy and it is therefore important to establish that thin films and bulk samples are indeed magnetically similar – as previously established for UPd_2Al_3 thin films. On XMaS we used a film of 1200Å thickness grown by MBE and performed x-ray resonant magnetic scattering with the photon energy tuned to the uranium M_4 absorption edge (E = 3.73keV).

Magnetic scattering has been observed at the (2 0.39 1/2) (Figure 1) and (1 1.39 1/2) positions proving that there is spatial magnetic order in the studied film with a propagation vector as reported of the bulk. Analysing the width of the magnetic peaks, we could establish a magnetic correlation length >800Å parallel to the growth axis and similar to the structural order. This suggests a magnetic and structural correlation, which extends over the complete film thickness. Nevertheless there is influence of the surface: we did not observe magnetic scattering peaks at (0.39 0 1/2), (0.61 0 1/2) and (1.39 0 1/2) positions, indicating that the magnetic domain with the moment direction perpendicular to the film surface is absent. Hence, the formation of a magnetic domain with a moment direction perpendicular to the film surface seems to be energetically unfavourable, possibly since it would imply an possibly since it would imply an uncompensated magnetic moment.

Our results confirm that indeed our thin film samples are magnetically equivalent to bulk samples and will now be used for tunnel spectroscopy experiments to investigate the details of superconductivity.

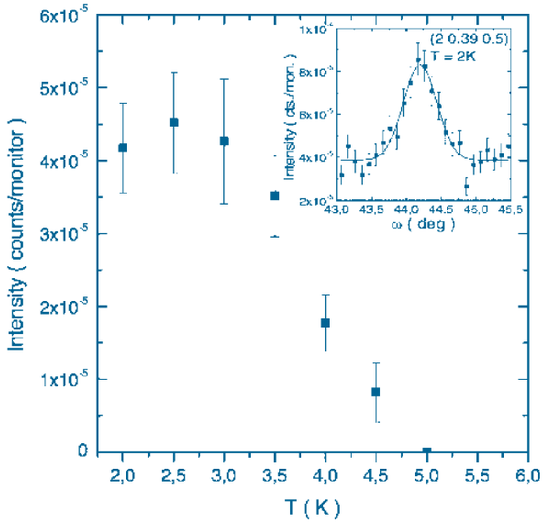

Figure 1: Temperature dependence of the integrated scattering intensity of the magnetic Bragg peak (0 0.39 1/2) (see inset).

Grazing incidence x-ray scattering from two-dimensionally patterned thin film nanoscale arrays

D.S. Eastwood, T.P.A. Hase, M. van Kampen, R. Bručas, B. Hjörvarsson, D. Atkinson, B.K. Tanner, P. Thompson and S.D. Brown – for further information contact T.P.A. Hase at University of Durham, Dept. of Physics, South Rd., Durham DH1 3LE, UK.
t.p.a.hase@durham.ac.uk

Large area arrays of nano-scaled objects are becoming increasingly important in both technological and fundamental studies. As in common with many systems, it is the distribution about the mean element size and repeat structure that determine the properties of the system. In order to understand the switching behaviour in systems composed of patterned magnetic media used in magnetic logic and storage devices, the mean and distribution of the element size and repeat pattern

need to be determined precisely. We have used grazing incidence x-ray scattering to probe the symmetry and dimensions of two dimensional written arrays. Here, we report non-resonant scattering measurements on two classes of two-dimensionally patterned sample. The first, was a 3mm square array of dots written by electron beam lithography/ion etching, into a multilayer of $[Ni_{80}Fe_{20}(3nm)/Al_2O_3(1.8nm)]_{x20}$ grown by DC/AC UHV based sputtering on a sapphire substrate. The second set of samples were 1mm square area, rectangular permalloy ($Ni_{80}Fe_{20}$) dot arrays, prepared on naturally oxidized Si (001) substrates by electron beam lithographic patterning and thin film deposition by thermal evaporation followed by chemical lift-off.

Exemplary transverse scans are shown in Figure 1 of a square array of $Ni_{80}Fe_{20}/Al_2O_3$ dots nominally 300 nm diameter and 600 nm pitch. As well as the diffuse scatter associated with the rough surface, additional peaks of coherent scatter, arising from the long range repeat structure appear symmetrically either side of the specular ridge at $q_x = 0$. Measurements from an AFM image (inset) showed that the element size was 305±10 nm diameter with a 610±10 nm pitch. Scanning electron microscopy measurements gave 330±20nm and 310±10nm diameter in the [10] and [01] directions respectively. The corresponding pitches were found to be 602±3nm and 606±2nm. The peak positions from the x-ray scans taken along the [10] and [01] directions are equal within the measurement precision and show that the lattice is square with a periodicity of 599±1 nm.

Figure 2 shows experimental and simulated rocking curves for an array of intentionally rough-edged Ni60Fe40 dots, orientated in the [11] in-plane direction. As in conventional diffraction, the satellite peak width is determined by the coherent scattering array area and the dispersion in the repeat structure. These two effects have a different variation with satellite order, but, in this case, the satellite peak widths were instrument resolution limited and fit closely the resolution function. We have based our simulation code using a semi-Kinematical approach. The two dimensional crystallography can be viewed by taking a series of scans, similar to those shown in figures 1 and 2, as a function of azimuth (Fig 3). In the samples studied a high degree of symmetry associated with a square lattice is seen. Where the lattice is of lower symmetry this map shows lower symmetry.

We have presented data on highly ordered systems which show exceptional long range order, and have shown that x-ray scattering, where the array structure is imaged in reciprocal space, can be a powerful tool in the precise determination of the long range order and element size. Similar experiments will provide quantitative determination of the in-plane coherence length of selfassembled arrays, a parameter critical to their exploitation in novel recording media and devices and one that cannot be obtained easily by imaging in direct space.

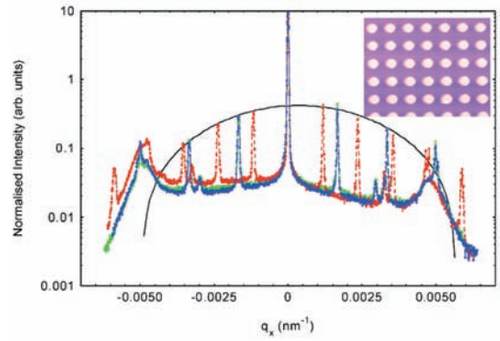

Figure 1: *Transverse scans at azimuth angles of 0° (green),45° (red) and 90° (blue) showing changing satellite positionsand a single envelope function. $Ni_{80}Fe_{20}$ / Al_2O_3 dot array.*

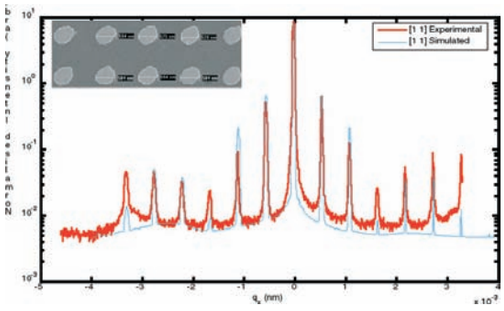

Figure 2: *Experimental and simulated rocking curves scans taken with the incidence plane in the [11] direction from a $Ni_{80}Fe_{20}$ array on Si (SEM image inset).*

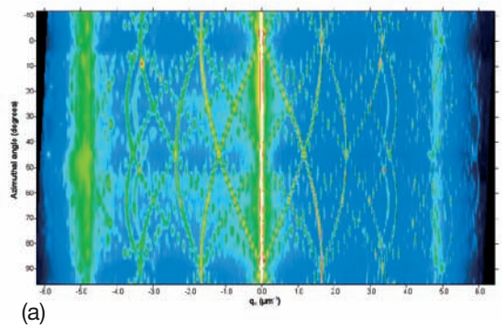

(a)

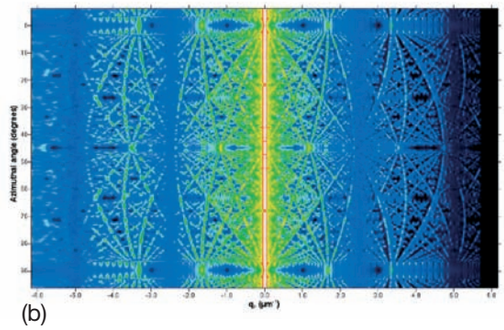

(b)

Figure 3 (a): *Experiment rotation map recorded at a scattering angle of 2.5° of an array of $Ni_{80}Fe_{20}$ / Al_2O_3 (Al_2O_3) multilayer pillars on a sapphire substrate. (b) Simulated map for a 600 nm square array of circular dots diameter 300 nm.*

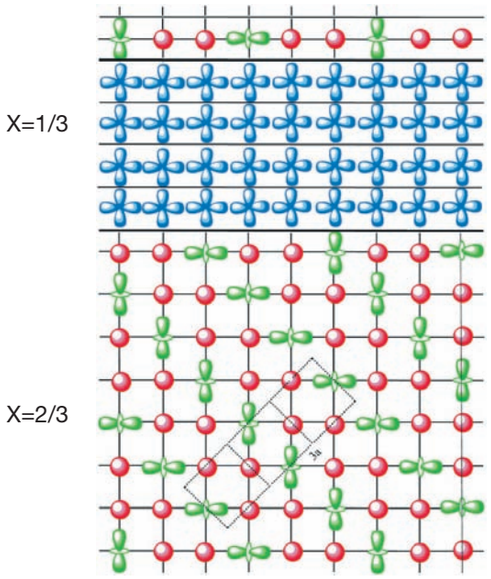

Figure 1: Schematic diagram of the e_g orbital states in $La_{1-x}Ca_xMnO_3$ [AF(x=2/3)/FM(x=1/3)] multilayers. Red circles represent Mn^{4+} ions, green figure-8's represent Mn^{3+}ions with ordering of the $(3z^2-r^2)$-type orbitals in the orthorhombic ac plane, and blue crosses represent disordered $(x^2-y^2)/(3z^2-r^2)$ orbitals from Mn^{4+}+/Mn^{3+} ions. Solid lines show the pseudo-cubic lattice along the (001) direction of growth and dashed lines the antiferro-orbitalorder unit cell in the ac *plane of the orthorhombic* (Pnma) *crystal structure.*

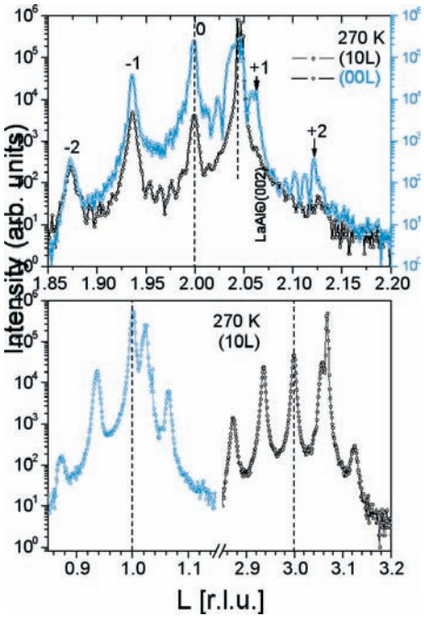

Figure 2: X-ray diffraction along the L direction in reciprocal space, where L denotes the continuous-valued coordinate of momentum transfer perpendicular to the surface of the sample. The spacing of the satellite peaks, Δ L=1/N, where N=number of layers in one AF/FM bilayer, gives the expected bilayer thickness Λ=6.1 nm when N is multiplied by the average lattice parameter of the pseudocubic unit cell (0.388 nm). Splitting of the $LaAlO_3$(00L) peaks indicates twining.

Exchange-bias in $La_{1-x}Ca_xMnO_3$ [AF/FM] multilayers

C. Christides, P.P. Deen, L. Bouchenoire, I. Margiolaki, K. Prassides – for further information contact: C. Christides at University of Patras, Dept Engineering Sciences, 26504 Patras, Greece.
christides@des.upatras.gr

Compositionally modulated $La_{1-x}Ca_xMnO_3$ [AF(x=2/3)/FM(x=1/3)] superstructures exhibit the exchange-bias effect below a blocking temperature T_B=80 K, well below the Néel (T_N=140 K) and charge-ordering (T_{CO}=250 K) temperatures of the antiferromagnetic (AF) layers. Resonant x-ray scattering at the Mn *K*-edge and diffraction measurements were performed on BM28 between 10 and 300 K in order to explore the influence of orbital ordering of the filled $Mn^{3+}e_g$ orbitals on the exchange-bias mechanism in $\{[La_{2/3}Ca_{1/3}MnO_3(3nm)FM]/[La_{1/3}Ca_{2/3}MnO_3(3nm)AF]\}_{15}$ multilayers. Figure 1 shows a simplified picture of the charge-ordered and orbital-ordered states in the AF layers. Figure 2 shows the superstructrure peaks measured from the multilayer at 270 K, revealing strong texture along the (00L) direction of film growth. Because of this effect, it was not possible to detect the peaks from the charge-ordered supercells, observed in the bulk AF structure. The diffraction patterns do not change down to 10 K.

Figure 3 shows the normalized peak intensities *I*(T)/*I*(10K), observed only for satellite peaks along the (*h*,0,1) and (*h*,0,2) directions. The decrease in intensity on heating above 80 K provides the first evidence that the exchange-bias mechanism may be related to resonant scattering. Complementary measurements of the energy dependence of the ($\sigma \rightarrow \sigma'$) and ($\sigma \rightarrow \pi'$) components further reveal an enhancement near the Mn K-absorption edge for both (1/201) and (1/202) reflections. Azimuthal angle dependence measurements performed for Ψ=0°, ±90° exhibit a characteristic periodicity as a function of Ψ. Additional experiments are planned in order to clarify the physical origin of these resonant scattering features.

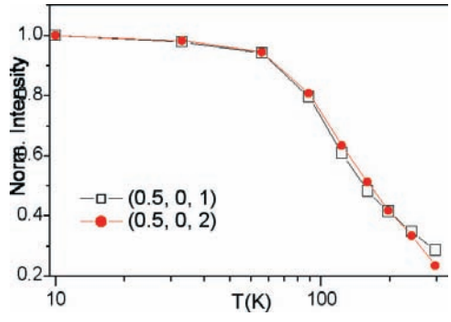

Figure 3: Temperature dependence of the scattering at the(0.5, 0, 1) and (0.5, 0, 2) reflections (semi-log plot) on resonance.

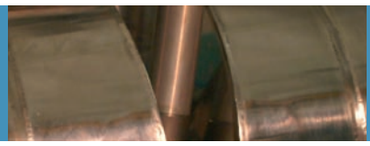

Structure and phase behaviour in prototypical helical hairy-rod polyfluorines

M. Knaapila, B.P. Lyons, T.P.A. Hase, L. Bouchenoire, P. Thompson, R.. Stepanyan, M. Torkkeli, and A.P. Monkman – for further information contact: Matti Knaapila at Department of Physics, University of Durham, South Road, Durham DH1 3LE, UK.

matti.knaapila@durham.ac.uk

Polyfluorines (PFs) are the most promising class of electroluminescent polymers for thin film applications, such as organic light-emitting diodes, which are to be used in the displays of digital cameras and mobile phones in place of conventional liquid crystal displays. The aim of our work is to progress the understanding of the complex hierarchical levels of solid state structure and phase behavior in a prototypical helical hairy-rod polyfluorene, poly[9,9-bis(2-ethylhexyl)-fuorene-2,7-diyl] (or PF2/6). This branched side chain containing polyfluorene undergoes a systematic intermolecular self-assembly and liquid crystalline phase behavior in combination with uniaxial and biaxial alignment (Figures 1 and 2). The latter processes yield full three-dimensional orientation of the crystallites and polymer chains. Also studied are the impact of the molecular structure and phase behavior on surface morphology, anisotropic film formation and, ultimately, the overall impact of these physical attributes on optical constants. This particular polyfluorene also represents a model system for demonstrating the applicability of mean-field theory in detailing the self-organization of aligned hairy-rod block copolymer systems. General guidelines of how molecular weight influences nanostructure, phase behavior, alignment, and surface morphology have also been formed. This ongoing study has, in part, been carried out at the XMaS beamline.

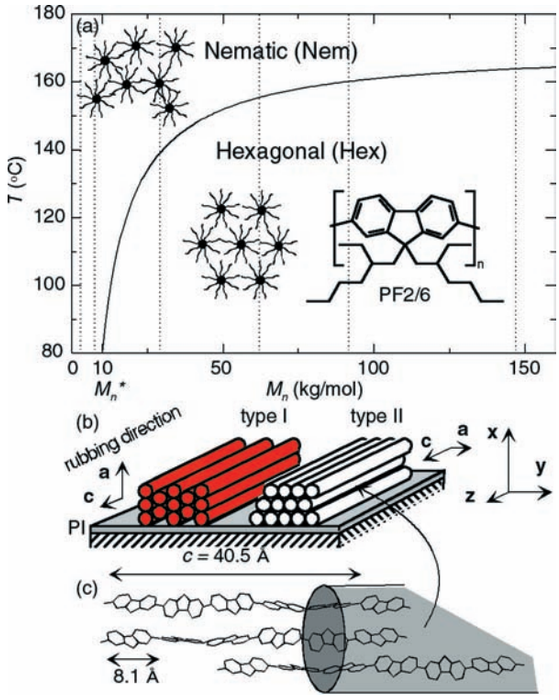

Figure 1. (a): The phase diagram and head-view schematics of nematic and hexagonal phases of PF2/6 as a function of M_n. M_n=104 g/mol. LMW: M_n<M_n*. HMW: M_n>M_n*. The schematics of (b) the crystallite types I (red) and II (white) and (c) molecular structure in aligned HMW films.*

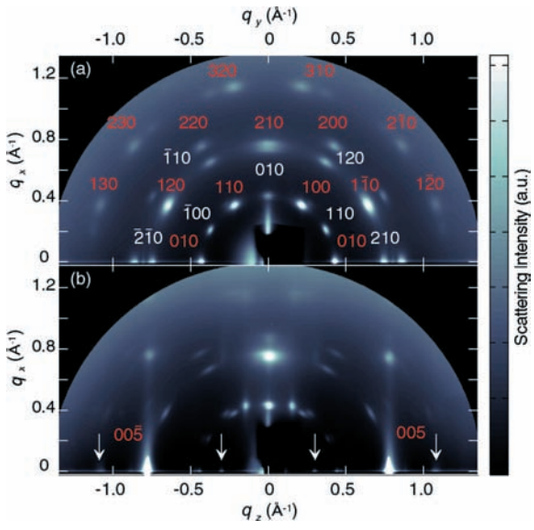

Figure 2: The 2D GIXD patterns of HMW PF2/6. (a) (xy0) plane. (b) (x0z) plane. Red and white indices correspond to the types I and II, respectively (cf. Figure 1b). The reflections which occur very close to 002 and 007 are indicated by the arrows.

Spectroscopic and theoretical investigation of the electronic and magnetic properties of the heavy rare earth metals

S.D. Brown, P. Strange, L. Bouchenoire, B. Zarychta, P. Thompson and D. Mannix – for further information contact S.D. Brown at XMaS, ESRF, Grenoble 38043.

sbrown@esrf.fr

We present a novel combination of x-ray resonant scattering from both ferromagnetic and antiferromagnetic phases, together with first-principles relativistic electronic structure calculations. Making judicious choices of scattering geometries, x-ray polarisations and temperature we are able to isolate 2p→5d electric dipolar scattering and observe both pure magnetic and magnetic-charge resonant interference scattering (Figure 1, see caption). The dipolar scattering resonances exhibit a two-peak structure with a splitting ranging from 4.5 to 6.4 eV. We demonstrate for the first time (Figure 2, see caption) that analysis of resonant interference scattering can provide a qualitative and quantitative description of band structure and magnetism using a model similar to that employed in XMCD. This provides a full interpretation of the experimental data including a new classification of some features of the spectra and an observation of a changeover from magnetism dominated by electron spin to magnetism dominated by electron orbital motion. ■

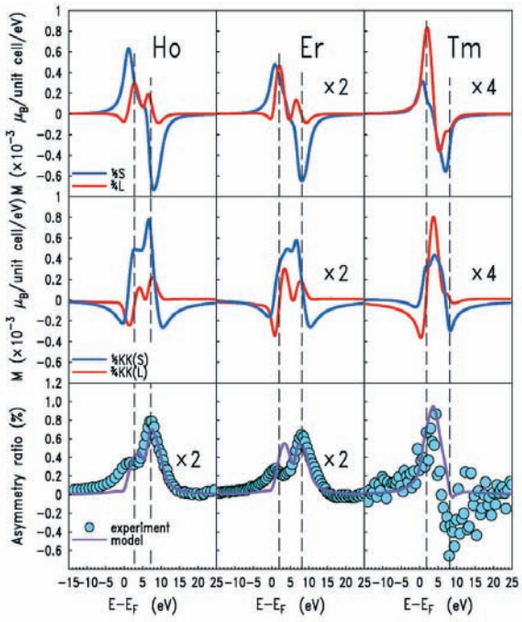

Figure 2: Modelling charge-magnetic interference scattering from Ho, Er and Tm. Convoluted spin and orbital 5d magnetisation densities (top panel) scaled as indicated for ease of comparison. Feature B in Fig. 1 correlates with an orbital peak around 2 eV above the Fermi level and corresponds to an orbital peak in the unoccupied 4f levels. The Kramers-Kronig transforms of the spin and orbital magnetisation densities (middle panel). The experimental and model asymmetry ratios (bottom panel). The changeover from spin dominant to orbital dominant magnetisations is apparent with increasing Z.

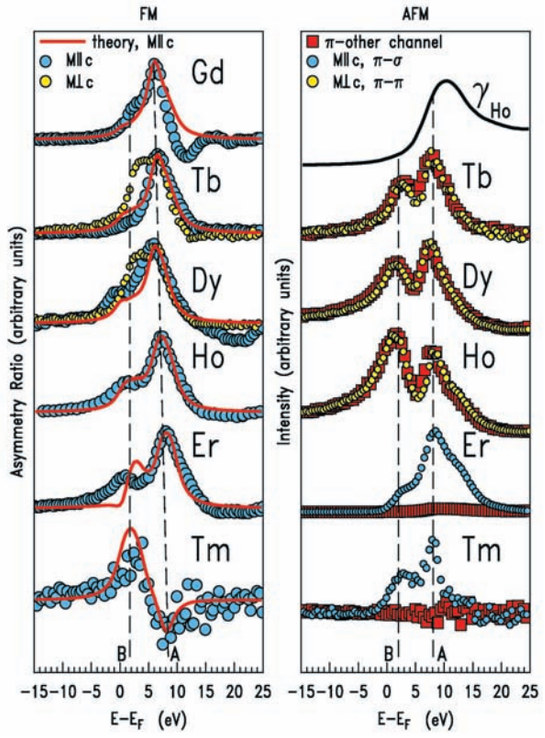

Figure 1: Left panel: Charge-magnetic interference scattering. Experimental data (cyan; c-axis, yellow; basal plane magnetisation, M), and first-principles scattering calculation (red). The agreement between experiment and c-axis magnetisation experiment is clear. The new XMaS 4 T superconducting magnet was used to pull the Tb/Dy moments along the c-axis resulting in qualitative agreement with the c-axis calculation.
Right panel: Antiferromagnetic scattering.
The approximated superposition of the ππ→σ and π→π scattering from Tb, Dy and Ho in the flat spiral phases indicates that both peaks are predominantly dipole in nature. The absence of π→π scattering from Er and Tm in CAM phases also indicates predominant dipole scattering. Again, c-axis moments agree with the calculation whereas basal plane moments (yellow) reveal an enhanced pre-peak (B) which in common with the model, increases in amplitude with increasing Z.

Investigating Multiferroics with RXS

D. Mannix, L. Bouchenoire, S. Brown, P. Thompson, D.F. McMorrow and A. Boothroyd for further information contact D. Mannix at XMaS, BM28, ESRF.

danny@esrf.fr

Magnetoelectric multiferroics, materials where magnetism and ferroelectricity coexist and interact, maybe of huge technological importance to the spintronics industry, where the sum of the combined physical properties offer a greater diversity in potential storage media than their individual parts. Recently, the $REMnO_3$ materials have attracted much scientific interest due to their gigantic magnetoelectric properties. For example, in $TbMnO_3$, the ferroelectric polarisation can be switched by applied magnetic fields, while in $HoMnO_3$, the magnetic coupling can be switched from antiferromagnet to ferromagnetic in applied electric fields. $TbMn_2O_5$ also exhibits a striking correlation between the magnetic and electric properties, the electric polarisation and dielectric constant undergo four separate transitions associated with anomalies in the magnetic susceptibility in a remarkable display of multiferroic behaviour. Moreover, the electric polarisation can be reversed by applying a moderate magnetic field (2 Tesla) at low temperature and a permanent imprint is left in the polarisation. This effect may have potential in new device applications such as magnetically recorded ferroelectric memory. A microscopic understanding of the magnetoelectric coupling is of fundamental importance to the technological advances of these materials. Resonant X-ray Scattering RXS is a powerful electron polarisation specific probe which may be exploited towards this goal.

Recent XMaS in-house time has been dedicated to RXS studies of $HoMnO_3$, with the aim of investigating the ferromagnetic flipping ratio in applied electric rather than the usual magnetic field. This work also represents a natural progression following previous in-house program of a systematic study of the ferromagnetism of the heavy rare-earth materials using RXS. These investigations have also enabled us to develop the sample environment to enable applied electric fields in conjunction with the new 4-Tesla superconducting magnet. To our knowledge, such a combined field sample environment is unique in synchrotron radiation.

In the first part of this study, we investigated the ferromagnetic response in $HoMnO_3$ in applied magnetic fields. The RXS energy and temperature responses are presented in figure 1, with the incident photon energy tuned to the Ho L_3 edge. The energy-line shape is essentially identical to that observed in pure Ho metal. Following these measurements, we have prepared a polished 0.8mm thick sample with gold electrodes deposited for the attachment of electrical contacts. Further experiments in applied electric and magnetic fields are planned for the next in-house experimental session at XMaS. ■

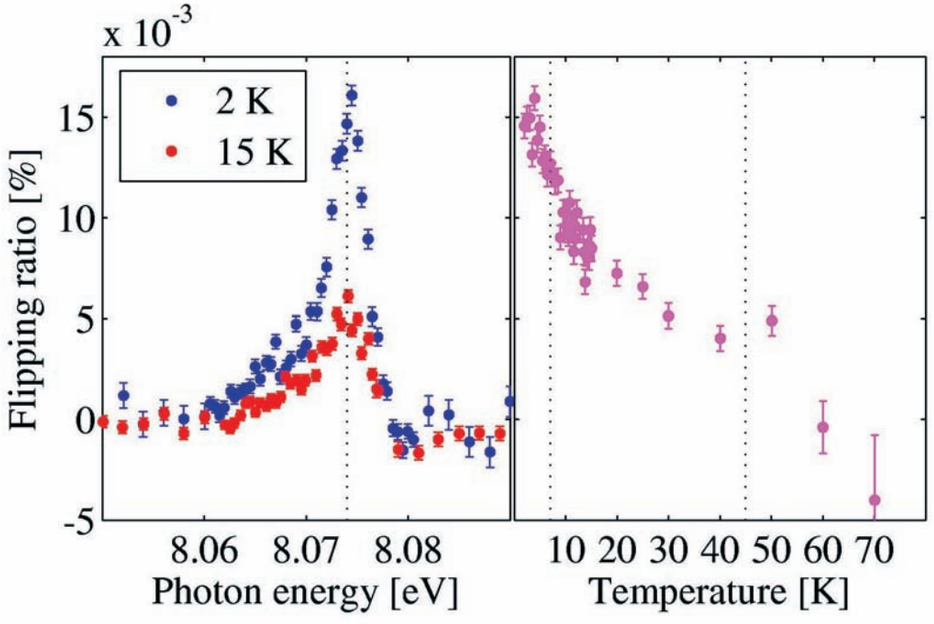

Figure 1: *The RXS ferromagnetic signal (flipping ratio) taken at the Ho L_3 edge in $HoMnO_3$ (left) and it temperature dependence (right).*

Please note

Some of the experimental reports in the previous pages are as yet unpublished. Please email the contact person if you are interested in any of them or wish to quote these results elsewhere.

Our web site

This is at:
http://www.esrf.fr/UsersAndScience/Experiments/CRG/BM28/
It contains the definitive information about the beamline and an on-line beamline manual.

Living allowances

These are still 55 euros per day per beamline user – the equivalent actually reimbursed in pounds sterling, of course. XMaS will continue to support up to 4 users per experiment if you can make a case for the presence of the fourth experimentalist. The ESRF hostel still appears adequate to accommodate all our users, though CRG users will always have a lower priority than the ESRF's own users. Do remember to complete the web-based "A form" requested of you when you receive the ESRF invitation, all attendees must be listed, since this informs the safety group of the attendees and is used to organise all site passes, meal cards and accommodation.

Beamline people

There have been no changes in the beamline staff since the last Newsletter.

Project Co-ordinator

David Paul, (dpaul@esrf.fr), is the person who can provide you with general information about the beamline, application procedures etc. David should normally be your first point of contact.

Beamline Scientists

Simon Brown (sbrown@esrf.fr), Danny Mannix (danny@esrf.fr) and Laurence Bouchenoire (boucheno@esrf.fr) continue as beamline scientists.

Technical Support

Paul Thompson (thompso@esrf.fr) continues to work on instrument development and provides technical support for the beamline. John Kervin (jkervin@liv.ac.uk), who is based at Liverpool University, provides further technical back-up and spends part of his time on-site at XMaS.

Project Directors

Malcolm Cooper (m.j.cooper@warwick.ac.uk) and Chris Lucas (clucas@liv.ac.uk) continue to travel between the UK and France to oversee the operation of the beamline. The administration for XMaS continues to be handled by Sandra Beaufoy at Warwick University (s.beaufoy@warwick.ac.uk).

The Project Management Committee

The current membership of the committee is as follows:

- Denis Greig (chair)
- Des McMorrow
- Peter Hatton
- Bob Cernik
- Colin Norris
- Simon Crook

Meeting twice a year, in addition to the above, the directors, the chair of the PRP and the beamline team are in attendance.

The Peer Review Panel

The current membership of the panel is as follows:

- Sean Langridge (chair)
- Paul Strange
- Nick Brookes
- Steve Collins
- Pam Thomas
- Helen Gleeson

In addition either Malcolm Cooper or Chris Lucas attend their meetings.

Housekeeping!!

We take some trouble to keep the beamline clean and tidy, please leave the beamline in the same state! At the end of your experiment samples should be removed from cryostat and other sample environment mounts, tools, etc returned to racks and unwanted materials disposed of in an appropriate manner. When travel arrangements are made, therefore, please allow additional time, at the cessation of beam, to effect a tidy-up.

PUBLISH PLEASE!!... ...and keep us informed

Although our list of papers reporting work on XMaS is growing we still need more of those publications to appear. We ask you to provide Sandra Beaufoy not only with the reference but also a preprint/reprint for our growing collection. Note that the abstract of a publication can also serve as the experimental report!

IMPORTANT!

When beamline staff have made a significant contribution to your scientific investigation you may naturally want to include them as authors. Otherwise we ask that you add an acknowledgement, of the form:

"This work was performed on the EPSRC-funded XMaS beam line at the ESRF, directed by M.J. Cooper and C.A. Lucas. We are grateful to the beam line team of S.D. Brown, D.F. Paul, D. Mannix, L. Bouchenoire and P. Thompson for their invaluable assistance, and to S. Beaufoy and J. Kervin for additional support." ■

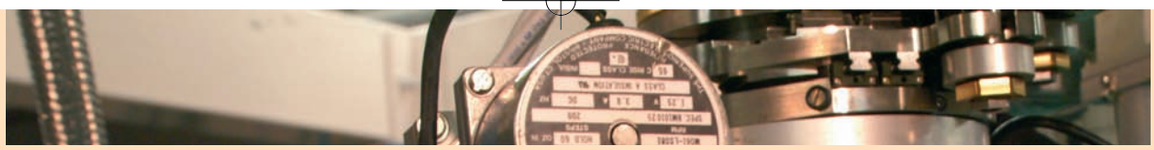

Guidelines
for Applying for Beam-time
at the XMaS beamline

Beamline Operation

The XMaS beamline at the ESRF, which came into operation in April 1998, has some 133 days of beam time available each year for UK user experiments, after deducting time allocated for ESRF users, machine dedicated runs and maintenance days. During the year, two long shut-downs of the ESRF are planned: 5 weeks in winter and 4 weeks in summer. At the ESRF beam is available for user experiments 24 hours a day.

Applications for Beam Time

Two proposal review rounds are held each year, with deadlines for submission of applications, normally, the end of March and September for the scheduling periods August to end of February, and March to July, respectively. Applications for Beam Time are to be submitted electronically (the paper versions are not acceptable) following the successful model used by the ESRF and ourselves. Please consult the instructions given in the ESRF web page:

www.esrf.fr
Follow the links: **"User Guide"**
And: **"Applying for Beam Time"**

Follow the instructions carefully – you must choose "XMAS-BM28" and "CRG Proposal" at the appropriate stage in the process. A detailed description of the process is always included in the reminder that is emailed to our users shortly before the deadline – for any problems contact D. Paul, as above.

Technical specifications of the Beamline and instrumentation available are described in the XMaS web page.

When preparing your application, please consider the following:

➡ All sections of the form must be filled in. Particular attention should be given to the safety aspects, and the name and characteristics of the substance completed carefully. Experimental conditions requiring special safety precautions such as the use of lasers, high pressure cells, dangerous substances, toxic substances and radioactive materials, must be clearly stated in the proposal. Moreover, any ancillary equipment supplied by the user must conform with the appropriate French regulations. Further information may be obtained from the ESRF Experimental Safety Officer, tel: +33 (0)4 76 88 23 69; fax: +33 (0)4 76 88 24 18.

➡ Please indicate your date preferences, including any dates that you would be unable to attend if invited for an experiment. This will help us to produce a schedule that is satisfactory for all.

➡ An experimental report on previous measurements must be submitted. New applications will not be considered unless a report on previous work is submitted. These also should be submitted electronically, following the ESRF model. The procedure for the submission follows that for the submission of proposals — again, follow the instructions in the ESRF's web pages carefully. Reports must be submitted within 6 months of the experiment.

➡ The XMaS beamline is available for one third of its operational time to the ESRF's user community. Applications for beamtime within that quota should be made in the ESRF's proposal round - Note: their deadlines are earlier than for XMaS! - 1st March and 1st September. Applications for the same experiment may be made both to XMaS directly and to the ESRF. Obviously proposals successfully awarded beamtime by the ESRF will not then be given beamtime additionally in the XMaS allocation.

Assessment of Applications

The Peer Review Panel for the UK-CRG considers the proposals, grades them according to scientific excellence, adjusts the requested beam time if required, and recommends proposals to be allocated beam time on the beamline.

Proposals which are allocated beam time must in addition meet ESRF safety and XMaS technical feasibility requirements.

Following each meeting of the Peer Review Panel, proposers will be informed of the decisions taken and some feedback provided. ■

XMaS Pluo B3, ESRF, BP 220, 38043 Grenoble Cedex, France
Tel: +33 (0)4 76 88 24 36 – Fax: +33 (0)4 76 88 24 55
Web page : http://www.esrf.fr/exp_facilities/BM28/xmas.html
Email: dpaul@esrf.fr

irma 04 76 53 24 94

THE UNIVERSITY of LIVERPOOL

XMaS the UK-CRG

is an EPSRC sponsored project

THE UNIVERSITY OF WARWICK